

## **IMPACT OF WATER REUSE PRACTICE ON SOIL CHARACTERISTICS, SALT MOVEMENT, AND YIELD FIELD EXPERIMENTS AND MODELLING IN THE NILE DELTA**

*D. Sabri<sup>1</sup>, B. Tischbein<sup>2</sup>, and R. Hinkelmann<sup>3</sup>*

<sup>1</sup>*Dahlia Sabri, KEO International Consultants, dsabri@uni-bonn.de*

<sup>2</sup>*Bernhard Tischbein, ZEF Bonn, Germany, tischbein@uni-bonn.de*

<sup>3</sup>*Reinhard Hinkelmann, TU Berlin, Germany, reinhard.hinkelmann@wahyd.tu-berlin.de*

### **ABSTRACT**

Improving water management depends on adequately understanding the water use practices, their functioning and their impacts, e.g. increase in soil salinity and water quality. Drainage water reuse has been practised since the seventies in Egypt. However, the sustainability of the water reuse practice has been threatened by the negative impacts of reused water on the soil-air-plant system. This study investigates the potential impacts of water reuse on soil characteristics and groundwater quality using experiments and modelling. An experiment was conducted in two fields in Mahalet Roh near Tanta city in the Nile Delta to study soil moisture distribution patterns and water-salt dynamics. The first field (F1) and the second field (F2) were irrigated with mixed water from the irrigation canal, and the surface drains electrical conductivity (EC) ranging between 1.0 to 1.4 dS / m while F1 had tile drains installed, whereas no tile pipes were installed in F2.

Results revealed that Electrical Conductivity (EC) values in F1 ranged between 2.3 - 3.5 dS / m, which is classified as slightly saline, while in F2, EC values ranged between 3.8 - 5.4 dS / m, indicating that the soils are moderately saline. Groundwater salinity was between 1.5 - 2.3 dS / m and 2.3 - 3.0 dS / m for F1 and F2, respectively. Water salinity in the tile network was found between 3.7 - 4.7 dS / m. The amount of water applied to F2 was higher than F1 by 7.5 %. When comparing the wheat crop yield, F2 was 16.6 % lower than F1. HYDRUS 2D software was used to model soil water movement and solute transport during the cropping season. The measured soil water content ( $\theta$ ) curves were in good agreement with the optimized soil water content. A mixing ratio of the canal and drainage water scenario was considered to simulate the effect of reuse water, presuming a mixing ratio of 1:3 of the canal to drainage water salinity. Overall, salinity distribution results for field F2 showed higher soil salinity than F1, indicating that salt accumulation increased in the absence of a drainage network under the same irrigation water salinity. Tile drains act as sinks that remove excess water from the root zone by enhancing leaching as a measure for soil salinity management in irrigation schemes.

**Keywords:** reuse practice, soil salinity, water quality, crop yield, modelling

### **1 INTRODUCTION**

The drainage network in the Nile Delta carries an annual discharge of about 17.5 BCM (billion cubic meters), from which 7.5 BCM are reused (officially and unofficially). Total cultivated lands are about 3.3 million hectares, of which about 35 % is affected by salinity (Rembold *et al.* 2000). Drainage Research Institute (DRI) reported that drainage water is becoming more saline in the Delta region; on average, salinity increased from 2.3 dS / m in 1995 to 3.2 dS / m in 2015. Salinity varies with location, whereas salinity ranges from 1.5 to 2.9 dS / m in the Nile Delta and continues to increase to a range between 5.4 to 9.4 dS / m in the northern part of the country.

However, water reuse plays a significant and essential role in plans to meet water requirements associated with future development; yet, reuse practices are constrained by availability and appropriate quality. Several threats to groundwater in the Nile Delta include contamination with

wastewater and pesticides and saltwater intrusion (Attwa et al., 2016). Due to salinity problems, the quality of reused drainage waters is of concern, particularly in arid / semi-arid regions, such as Egypt. Groundwater quality in the Nile system is reasonable; however, pollution has affected some shallow groundwater bodies. Almost 20 % of groundwater in the Nile aquifer does not meet drinking water standards, especially at the fringes with little or no protective clay cap (Negm et al., 2018).

The economics of drainage water reuse and its financial feasibility are another concern. However, although the government plans to establish treatment plants for the villages of the Nile Delta, this could take a long time to be implemented and depend mainly on the availability of financial resources. The extension of water reuse cannot be postponed till this problem is solved. The government plans for this expansion are based on a data availability level which needs to be improved by further analyses. There is also a need to become more detailed to assess and show the proposed schemes' feasibility and sustainability. With the limited Nile water supply, the ongoing expansion of cultivated land will be influenced by climate change, and freshwater availability will become scarcer for cultivated land, particularly in the Nile Delta area. The Ministry of Water Resources and Irrigation (MWRI) is the key governmental body which plays a major role in the management and development of the water sector. MWRI has been adopting and formulating several policies and plans to increase the water supply in the future. Water policy in 1975 referred to the role and importance of water in national development.

The policy suggested opting for drainage water reuse to increase water availability. Expansion of drainage reuse is constrained by other factors such as the minimum drainage outflow requirements, pollution of drainage water, and institutional capacities. Another constraint expected to reduce drainage water reuse in the Delta region is the increased waterlogging combined with an increase in soil salinity due to poor agricultural practices and mismanagement of irrigation systems (MWRI, 2014). The Egyptian guidelines aim at protecting the waterways from pollution. Law 48/1982 on "Protection of the Nile River and its Waterways from Pollution" controls the discharge of different effluents into the Nile and waterways. Law 12/1982 regards the irrigation and drainage, ministerial decree 8/1983 on law 48/1982 concerns the reuse of drainage water, and ministerial decree 44/2000 regards the amendment of law 93/1962 on the drainage of liquid wastes (MWRI, 2016; Ritzema *et al.*, 2011; MALR, 2012a). Drainage reuse is practised in the Delta region through twenty-two main drainage reuse stations. The system provides about 4 BCM / yr of drainage water mixed with fresh water from the main canals.

Advanced water management is needed as a promising strategy to cope with this challenging water situation. Water reuse and groundwater utilization are considered measures to compensate for future demand-supply gaps. Water shortage has been experienced during the last decades as the cultivated area increased from 6.0 to 8.8 million feddan<sup>1</sup> (3.3 million hectares), considered around 3.6 % of the country's land area. Of this agricultural land, 90 % (8.0 million feddan) is in the Nile Valley and Delta, while the remaining 10 % (0.8 million feddan) is rainfed in other parts of the country or the oases. Of the total area of the Nile Valley and Delta, about 6 million feddan are old lands. The remaining 2.8 million feddan are newly reclaimed lands.

At various locations of irrigation systems, non-uniform water distribution causes over-irrigation in upstream and water shortage at the canal tail, which creates the need to supplement the water supply by reusing water. Farmers at the canal tail, who face water deficits, compensate for the deficit of conventional irrigation water by reusing water from neighbouring drains, regardless of the pollution level in drain water. This uncontrolled water reuse impacts to soil, groundwater, crops and public health. This problem is expected to spread due to the expansion of water reuse, growing population, and surface and groundwater quality degradation. Potential conflicts between water reuse and other

---

<sup>1</sup> 1 feddan = 0.42 hectares = 1.038 acres



Reference evapotranspiration, calculated according to the Penman-Monteith equation (Allen *et al.*, 1998), is relatively high during summer, with about 6.3 mm / d in June and about 1.9 mm / d in December. The annual mean pan evaporation is about 5.0 mm / d. The relative humidity is relatively low in summer and high during winter, about 50 % in May and 71 % in January. Most of Egypt is a hyper-arid country (Awadallah *et al.*, 2017); rain is scarce and falls along the northern coastal zone (parallel to the Mediterranean) (Abdel-Maksoud, 2018).

Figure (2, left) shows soil texture of the upper layer in field F1 is clay (0 – 60 cm), the successive layer (60 - 100 cm) is clay loam, and in the subsoil layer, sand fraction increases, so it classified as sandy clay loam. While for F2, the upper layer of the fields is clay (0 – 80 cm), the following layer (80 -120 cm) is clay loam, while the subsoil layer is classified as sandy clay loam due to the increase in sand fraction (Figure 2, right).

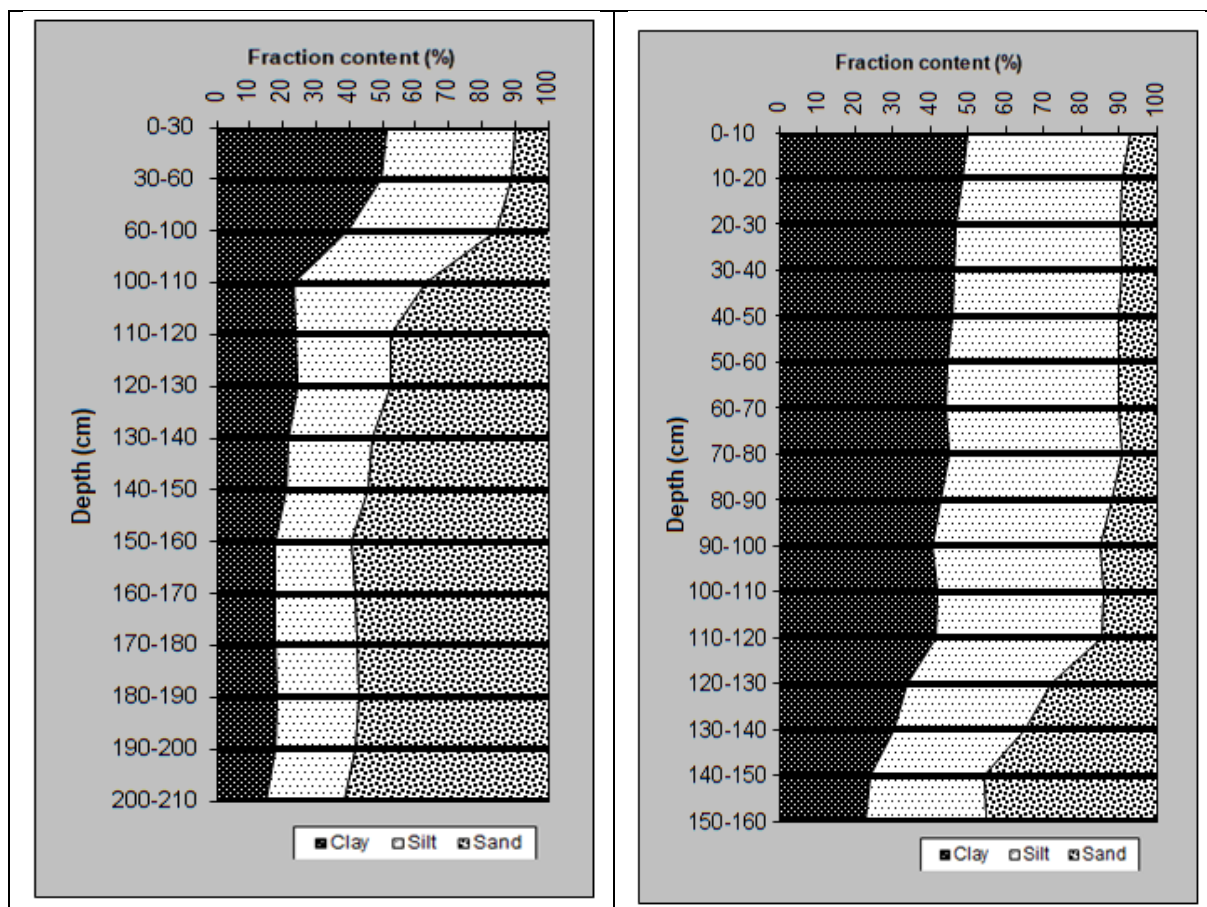


Figure 2. Soil profile analysis of F1 (left) and F2 (right)

## 2.2 Design of Research

A field experiment was carried out during the wheat growing season. Fields of similar or nearly the same size were selected, and each experimental field was divided into subplots to establish representative samples. To analyze water reuse impacts on soil salinity and groundwater quality, two fields were irrigated with mixed water from the irrigation canal and the surface drain characterized by electrical conductivity (EC) ranging between 1.0 to 1.4 dS / m. The ground elevation of the study area is almost flat, ranging about 9 to 15 m above mean sea level from north to south, respectively, with calcareic fluvisols and alluvium deposits from the Nile.

F1 was cultivated with rice at the beginning of the field investigation, and wheat was grown during winter. While F2 was cultivated with clover at the beginning of the field investigation, wheat was

cultivated during the winter season. The soil texture in the area is clay. The soil is saline-alkali with pH ranges from 7.91 to 8.26. This could be due to the high rates of evaporation coupled with minimal precipitation. In addition, abundant reuse of mixed water in irrigation enhances salt accumulation in the soil, especially in poor drainage system design and performance. The soil structure is angular to sub-angular blocks with clay like texture. Planting was carried out in late October / early November. The rows were 0.8 m apart, and the plant density was 75 000 plants/ha. The fields were irrigated by flood irrigation. Farmers apply inorganic fertilizers and organic fertilizers (manure); for each hectare of wheat, they apply 250 - 450 kg of inorganic fertilizers and 100 kg of manure. These amounts are typical and exceed the crop requirements. Inorganic fertilizers are 110 kg of potassium sulphate, 70 kg of superphosphate and 285 kg of ammonium nitrate. Fertilizers were applied two times in the field. Harvest was done manually.

For modelling water flow and solute transport, HYDRUS 2D (Simunek *et al.*, 2002) was selected for application in the study. HYDRUS 2D was chosen because it is a user-friendly model that can simulate and estimate water and salt balances under shallow groundwater and solute transport; moreover, it is widely used by researchers and scientists worldwide, so it is well-documented and updated regularly. HYDRUS2D was used to study (i) the vertical movement of applied irrigation water and solute transport in the unsaturated zone and (ii) the horizontal movement and transport within the groundwater.

## 2.3. Experimental and Numerical Methods

### 2.3.1 Soil and water sampling monitoring scheme

Representative soil horizons were sampled from pits to determine soil hydrophysical and chemical properties. Soil pits were excavated. Each pit is 2 m wide and 1.5 m deep. Soil samples were taken by auger at different depths of 0 - 30 cm, 30 - 60 cm, 60 - 100 cm and 100 -150 cm. Soil samples were taken to the laboratory for analysis to acquire the physiochemical properties of the soil. The samples were weighed for their initial wetness and later dried in the oven at 105 °C for 24 to 48 hours to remove inter-particle absorbed water.

Equation (1) was used to measure the water content as the difference between the wet and the dry weights having the mass of water held in the initial sample:

$$\theta_g = \frac{M_{\text{wet}} - M_{\text{dry}}}{M_{\text{dry}}} \quad (1)$$

where  $\theta_g$  [ $\text{cm}^3/\text{cm}^3$ ] represents soil moisture water content on weight base,  $M_{\text{wet}}$  [g] is the mass of the wet sample, and  $M_{\text{dry}}$  [g] is the mass of the dried sample.

Physical properties comprise soil moisture, permeability, porosity, bulk density, infiltration rate, and soil texture. The electrical conductivity of soil is highly associated with the total solute concentration of dissolved salts (i.e., salinity). Soil salinity is a measure of dissolved salts in the soil and measured by electrical conductivity, which indicates the presence of significant dissolved inorganic solutes (e.g.,  $\text{Na}^+$ ,  $\text{K}^+$ ,  $\text{Mg}^{2+}$ ,  $\text{Ca}^{2+}$ ,  $\text{Cl}^-$ ,  $\text{HCO}_3^-$ ,  $\text{NO}_3^-$ ,  $\text{SO}_4^{2-}$  and  $\text{CO}_3^{2-}$ ) (Richards, 1954). Total carbonates were determined volumetrically using Collin's calcimeter, following Piper (1950). Following Page (1982), soil pH and the electrical conductivity (EC) in  $\text{dS} / \text{m}$  were determined. The total soluble ions were measured in soil paste using an electrical conductivity bridge, and soluble anions and cations were determined titrimetrically by the versenate method, while  $\text{Na}^+$  and  $\text{K}^+$  were measured using a flame photometer. The chromic acid method of Walkley and Clack determined organic matter content, following Page (1982). The soil data are used to describe the hydrodynamics of the study area. In addition, they serve as input parameters for the model.

Field water sampling (irrigation, drainage, and groundwater) was done to determine the impact of reused irrigation water. Shallow observation wells were installed in the fields to provide the data needed about groundwater levels. Pipes were slotted 50 cm from the bottom end and covered with a filter to allow only water to enter. Pipes were 3.0 m long and were installed in the fields. The piezometers were left to stabilize for a minimum of 24 hours. The length from the soil surface to the top of each pipe was measured to ensure accurate measuring of groundwater levels. Groundwater water levels were recorded and monitored manually using a meter. Irrigation and drainage water samples were collected from canals, collectors and drains 30 cm below the water surface (Hutton, 1983). Water samples were collected before, in between and after each irrigation event to enable a good representation of water quality analysis.

Water samples were canned into uncontaminated bottles and then taken to the laboratory to be analyzed to obtain the chemical properties of the water. Two trapezoidal sharp-crested (Cipoletti) weirs were constructed to measure the water discharge. The discharge through a Cipoletti can be calculated as shown in equation (2):

$$Q=1.84 \cdot L \cdot H^{1.5} \quad (2)$$

Where Q is discharge [ $m^3 / s$ ], L is the bottom of notch width [m], and H is the head above the bottom of opening [m]. Fields were irrigated five times during the cropping season, in addition to planting irrigation, so discharge measurements were taken every minute in the fields during each irrigation event.

### 2.3.2 Numerical modelling of water flow in porous media

To simulate the impact of reuse water on the soil salinity and shallow groundwater quality, HYDRUS 2D numerically solves the Richards equation for saturated–unsaturated water flow (Equations 3, 4, 5 and 6) and the Fickian-based advection–dispersion equation for solute transport (Simunek *et al.*, 1998b) (Equation 7). The flow equation incorporates a sink term to account for water uptake by plant roots:

$$\frac{\partial \theta}{\partial t} = \frac{\partial}{\partial x_i} \left[ K \left( K_{ij}^A \frac{\partial h}{\partial x_j} + K_{ij}^A \right) \right] - S \quad (3)$$

In the two-dimensional flow scenario,  $K$  is the unsaturated hydraulic conductivity given by Equation (4):

$$K(h, x, y, z) = K_s(x, y, z) K_r(h, x, y, z) \quad (4)$$

Where  $\theta$  is the volumetric soil water content [ $cm^3 / cm^3$ ],  $h$  is the soil-water pressure head [cm],  $x_i (i=1,2)$  are the spatial coordinates [cm],  $t$  is time [day],  $K_{ij}^A$  is components of a dimensionless anisotropy tensor  $K^A$ ,  $K$  is the unsaturated hydraulic conductivity function [cm / s],  $z$  is the gravitational head as well as the vertical coordinate [cm] (upwards direction is positive),  $S$  is a sink term for soil water extraction rate by plant roots [1/ s].  $K_r$  is the relative hydraulic conductivity [-], and  $K_{sat}$  is the saturated hydraulic conductivity [m/s] (Šimunek *et al.*, 2008).

$$\theta(h) = \begin{cases} \theta_r + \frac{\theta_s - \theta_r}{[1 + |\alpha h|^n]^m} & h < 0 \\ \theta_s & h \geq 0 \end{cases} \quad (5)$$

$$K(h) = K_s S_e^l \left[ 1 - \left( 1 - S_e^{1/m} \right)^m \right]^2 \quad (6)$$

$$S_e = \frac{\theta - \theta_r}{\theta_s - \theta_r} = [1 + |\alpha h|^n]^{-m} \quad (7)$$

Where  $\theta(h)$  is the volumetric water content related to the pressure head,  $\theta_r$  and  $\theta_s$  are residual and saturated water contents [ $\text{cm}^3/\text{cm}^3$ ], respectively,  $h$  is matrix potential [m],  $\alpha$  [ $1/\text{cm}$ ],  $n$  and  $m$  are shape parameters,  $K(h)$  is the hydraulic conductivity related to pressure head [ $\text{cm}/\text{day}$ ],  $K_s$  is the saturated hydraulic conductivity [ $\text{cm}/\text{day}$ ],  $S_e$  is effective saturation,  $l$  is a pore connectivity parameter,  $m = 1 - 1/n$  when  $n > 1$ .

$$\frac{\partial nc}{\partial t} = \frac{\partial}{\partial x_i} \left( nD_{ij} \frac{\partial c}{\partial x_j} \right) - \frac{\partial q_i c}{\partial x_i} - SC_s \quad (8)$$

where  $C$  is the solute concentration [ $\text{g}/\text{l}$ ],  $D_{ij}$  is the hydrodynamic dispersion coefficient, [ $\text{cm}^2/\text{day}$ ],  $q_i$  is the volumetric flux density (Darcy flux) [ $\text{cm}/\text{day}$ ],  $t$  is time [day],  $x_i$  ( $i=1,2$ ) are the spatial coordinates [cm], the parameter  $D$  was taken as  $= Kq_i$  where  $K$  is the dispersivity [cm].  $S$  is the sink term of the water flow in the Richards equation [ $1/\text{s}$ ], and  $C_s$  is the concentration of the sink term [ $\text{mg}/\text{l}^3\text{s}$ ].

HYDRUS 2D includes the Levenberg-Marquardt (LM). The two-dimensional part of the program also includes a Marquardt-Levenberg-type parameter optimization algorithm for inverse estimation of soil hydraulic and/or solute transport and reaction parameters from measured transient or steady-state data for two-dimensional problems (Šimůnek *et al.*, 2006). The governing flow and transport equations are solved using a Galerkin-type linear finite element method.

Meteorological data were used to estimate average monthly potential evapotranspiration values with the modified Penman equation (Allen *et al.*, 1998) using recorded meteorological data processed by the FAO CROPWAT model. Meteorological data were collected from the Tanta station, nearest the study area, and crop coefficient ( $K_c$ ) values for wheat (FAO, 1998) were used to convert these values into crop-specific evapotranspiration estimates. The calculated daily atmospheric boundary condition is defined as the upper boundary condition and was specified as the maximum value for the time-dependent atmospheric surface flux boundary condition in HYDRUS 2D. The vertical and lower boundary, 6 m below the water table, was set to be no-flux boundaries so that no external flux could interfere with the total flux entering the fields. The vertical boundary, where the irrigation water canal is in the saturated zone, was defined as a constant pressure head boundary calculated from the water level in the canal. Feddes *et al.* (1978) suggested a water stress response function, which is represented as a sink term in the Richards equation to account for root water uptake

### 3 RESULTS AND DISCUSSIONS

Soil salinity in both fields could be defined as sodium chloride and calcium chloride type of salinity. The extracted solutions from soils, if total salt concentration (i.e. electrical conductivity of soil (EC)) exceeds 2 dS / m (at 25 °C), can be categorized as salt-affected (e.g. Abrol *et al.*, 1988). However, if the soil extract has an electrical conductivity of more than 4 dS / m, the soil can be categorized as saline soil. The measured soil salinity in F1 showed that the EC ranged from 2.3 to 3.4 dS / m putting them in the slightly saline category. While the EC of soil in F2 varied from 3.8 to 5.1 dS / m, this indicates that the soils of this area are moderately saline. Figure 5 shows soil salinity values after irrigation in the fields.

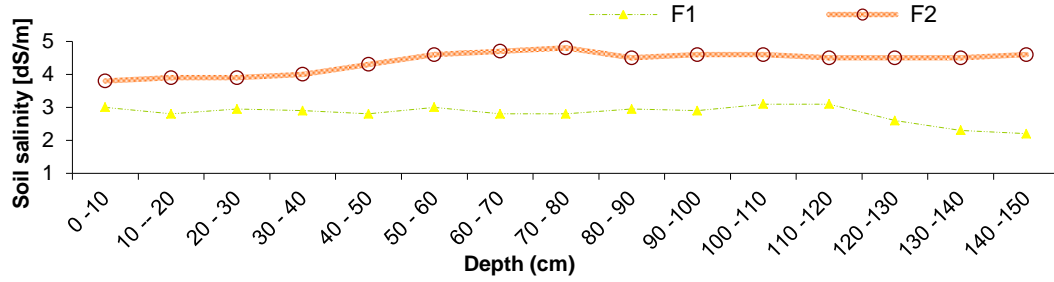


Figure 5. Soil salinity after irrigation in F1 & F2

Groundwater salinity was monitored during the winter season before cultivation. After that, before, in between and after each irrigation event. Figure 6 shows the salinity recorded in each field obtained from five monitoring wells dug in each field for groundwater sampling. The data of F1 groundwater salinity showed ranges between 1.5 and 2.30 dS / m, while in F2 samples analysis showed 2.28 to 2.99 dS / m.

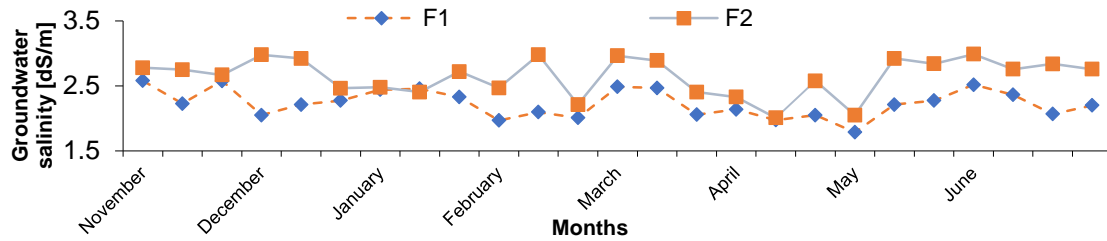


Figure 6. Groundwater salinity measurements

Data analysis showed that sodium ( $\text{Na}^+$ ), calcium ( $\text{Ca}^{2+}$ ), chloride ( $\text{Cl}^-$ ), and sulphate ( $\text{SO}_4^{2-}$ ) are the dominant anions and cations in the soil of the two fields. Figures 3 and 4 show the constituent of the cations and anions before irrigation (1), after irrigation (2) and between irrigation events (3) in the two fields. In field F1, where irrigation is done with fresh canal water mixed with drainage water and a drainage network, sodium, calcium, and chloride prevailed.  $\text{Na}^+$  content was 15.5, 33.4 and 19.2 meq / l,  $\text{Cl}^-$  was 18, 34.7 and 22.5 meq / l, magnesium ( $\text{Mg}^{2+}$ ) content was 1.8, 1.7, and 2 meq / l,  $\text{Ca}^{2+}$  content was 2.9, 2.7 and 3.2 meq / l, potassium ( $\text{K}^+$ ) content was 0.5, 0.2 and 0.6 meq / l,  $\text{SO}_4^{2-}$  was 0.8, 1.3 and 1.5 meq / l and bicarbonate ( $\text{HCO}_3^-$ ) was 1.5, 2 and 1.5 meq / l before irrigation, after irrigation and between irrigation events, respectively. In field F2, where irrigation is done with fresh canal water mixed with drainage water and without a drainage network, the anions and cations content were noticeably higher than in F1.  $\text{Na}^+$  content was 31.1, 36.1 and 32.5 meq / l.  $\text{Cl}^-$  was 33.2, 42.1 and 35.4 meq / l;  $\text{Mg}^{2+}$  content was 2.7, 3.8, and 2.5 meq / l;  $\text{Ca}^{2+}$  was 3.3, 6.3 and 4.3 meq / l.  $\text{K}^+$  was 0.5, 0.8 and 0.8 meq / l,  $\text{SO}_4^{2-}$  was 2.4, 2.6 and 2 meq / l and  $\text{HCO}_3^-$  was 2.5, 2.3 and 2.8 meq / l before irrigation, after irrigation and between irrigation events, respectively.

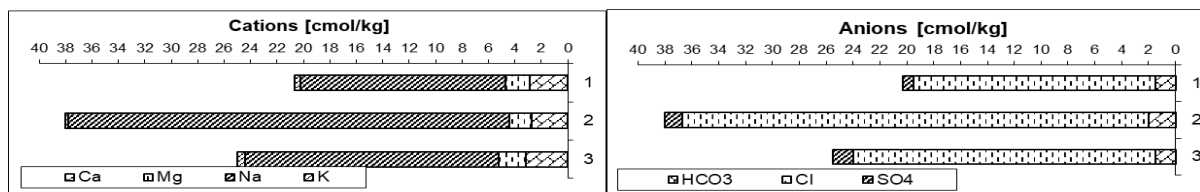


Figure 3. Ion concentration in F1



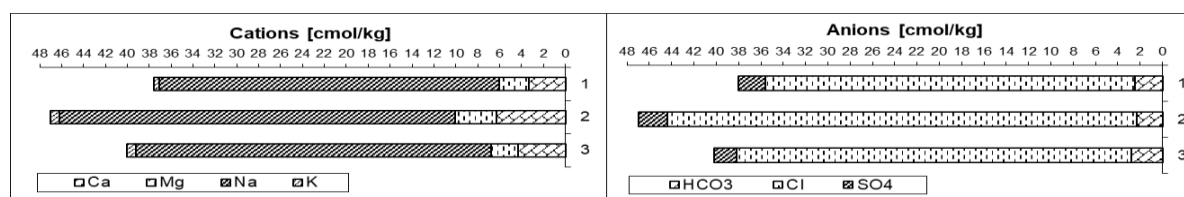


Figure 4. Ion concentration in F2

During the cropping season, the amount of applied water for irrigation was about 648 and 696 mm for F1 and F2, respectively. This makes the amount of water applied to F2 higher by 7.5 % than F1. Wheat is considered a moderately salt-tolerant crop; however, wheat can face problems during germination if soil salinity (EC) exceeds 4 dS / m in the upper soil layer. The yield of winter wheat decreases due to salinity is 0 % at EC 6.0, 10.0 % at 7.4, 25 % at 9.5, 50.0 % at 13.0 and 100.0 % at EC 20 dS / m (FAO-61, 2002).). The yields were about 2.2 and 1.75 tons for F1 and F2, respectively, i.e., the yield of wheat crops in F2 was 16.6 % lower than in F1.

The groundwater table was monitored every three or four days. Generally, the groundwater table noticeably fluctuated in the fields before irrigation, between irrigation events and immediately after irrigation. In F1, a drainage network was installed, groundwater table fluctuated from 190 to 204 cm, 175 to 188 cm and 161 to 172, before irrigation, between irrigation and immediately after irrigation, respectively. In F2, where no drainage network was installed, the groundwater table fluctuated from 106 to 118 cm, from 89 to 99 cm and from 73 to 85 cm, before irrigation, between irrigation and immediately after irrigation, respectively.

HYDRUS applies an indirect method to estimate the unsaturated soil hydraulic parameters from initial values. HYDRUS 2D uses soil hydro-physical characteristics data to estimate parameters for the functions  $\theta(h)$  and  $K(\theta)$  (Equations 3, 4 and 5). Estimates of  $\theta_s$ ,  $\theta_r$ ,  $\alpha$ ,  $n$  and  $l$ , and the saturated hydraulic conductivity  $k_s$  for each soil layer were used. The longitudinal dispersivity ( $D_L$ ) value was taken to be equal to one-tenth of the domain depth, while transverse dispersivity ( $D_T$ ) was taken equal to 0.1  $D_L$ , as suggested by Anderson (1984) and Cote *et al.* (2001). Table 1 lists the Genuchten–Mualem analytical model parameters for the soil water retention and conductivity curves.

Table 1. Genuchten–Mualem analytical model parameters

Depth [cm]	$\theta_{res}$ [cm <sup>3</sup> /cm <sup>3</sup> ]	$\theta_{sat}$ [cm <sup>3</sup> /cm <sup>3</sup> ]	a -	n [l/cm]	$K_s$ [cm/hr]	l -	Particle size distribution, %			Lithology
							Sand	Silt	Clay	
F1										
0-30	0.087	0.514	0.0044	1.58	5.98	0.50	9.6	38.5	51.9	C
30-60	0.088	0.515	0.0030	1.29	6.48	0.50	10.8	39.3	49.9	SiC
60-100	0.099	0.494	0.0417	1.02	11.42	0.50	15.2	45.4	39.4	SiCL
100-130	0.090	0.460	0.0405	1.19	13.46	0.50	47.2	29.1	23.7	L
130-150	0.062	0.407	0.0179	1.42	25.36	0.50	54.4	24.8	20.9	SaCL
150-200	0.052	0.378	0.0390	1.44	18.59	0.50	58.5	24.3	17.2	SaL
200-600	0.094	0.447	0.0076	1.26	9.05	0.50	17.0	33.6	49.4	C
F2										
0-10	0.078	0.478	0.0078	1.39	5.90	0.50	6.9	43.0	50.1	SiC
10-30	0.076	0.473	0.0023	1.21	6.52	0.50	9.3	42.9	47.8	SiC
30-60	0.072	0.459	0.0055	1.08	7.37	0.50	9.7	44.7	45.6	SiC
60-90	0.070	0.454	0.0018	1.12	9.55	0.50	10.5	45.4	44.1	SiC
90-120	0.066	0.441	0.0013	1.48	10.00	0.50	14.4	44.2	41.4	SiC
120-140	0.060	0.428	0.0118	1.70	14.53	0.50	31.3	36.45	32.25	CL
140-160	0.055	0.421	0.0233	1.71	31.66	0.50	45.25	31.15	23.6	L
160-600	0.074	0.464	0.0045	1.44	10.73	0.50	14.5	36.5	49.0	C

HYDRUS creates a correlation matrix that indicates the degree of correlation between the fitted coefficients. The domain to model the study fields included a cross-section of the irrigation water canal and a longitudinal section of the irrigated studied fields. Soil hydraulic and transport parameters were calibrated and validated using field data collected during the study. RMSE values were calculated, and regression analysis of the observed versus the fitted data was done. The closer the RMSE values are to zero, the better the model predicts the measurements. The soil pF-curve was determined in the laboratory using the pF range between 0.1 - 15 bar for each undisturbed soil sample. Measured and simulated soil water content ( $\theta$ ) in fields F1 and F2 are represented in Figure 7.

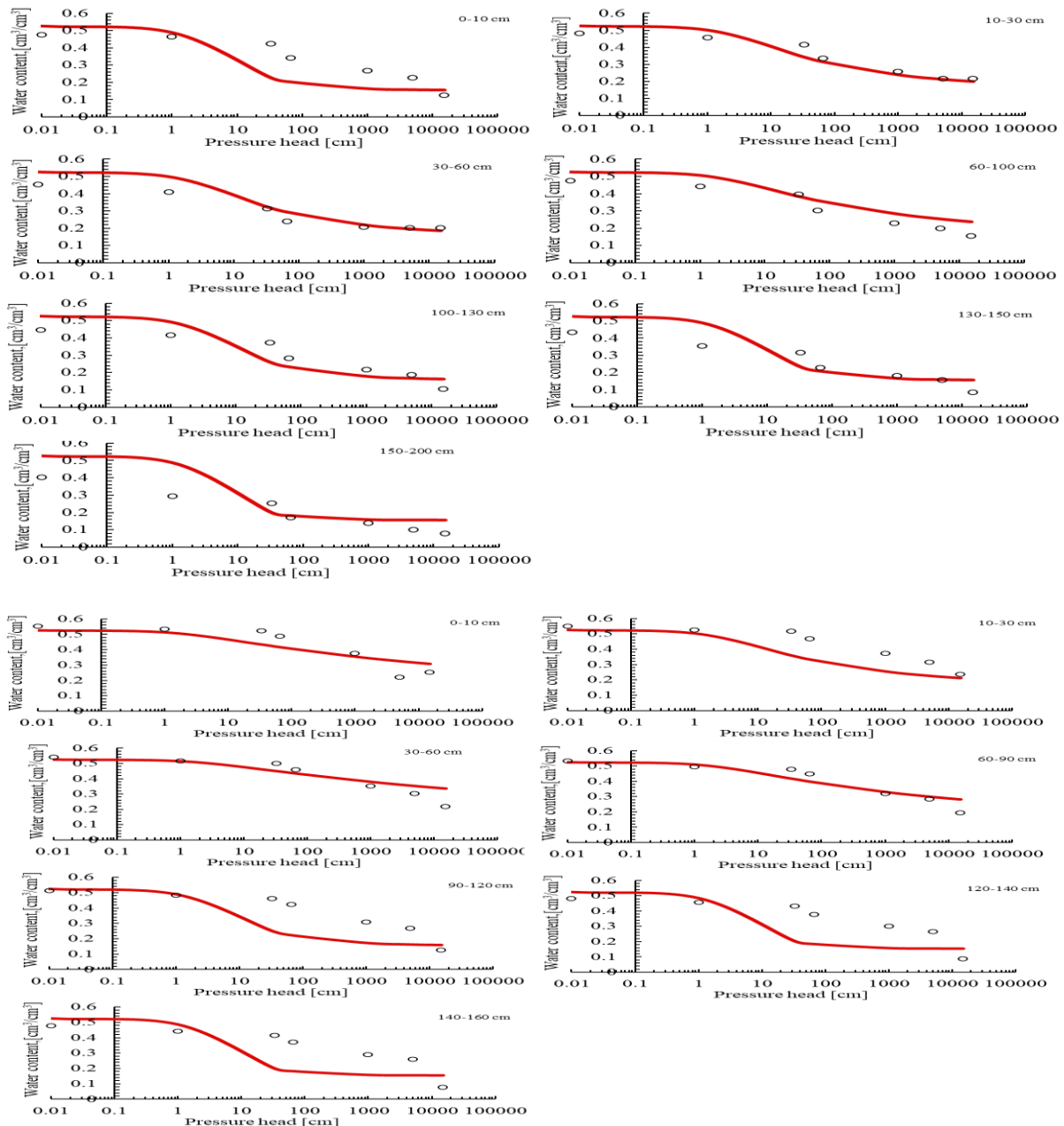


**Figure 7. Measured (dots) and simulated (solid line) soil moisture content ( $\Theta$ ) at different pressure heads ( $\psi$ ) for different soil layers of fields F1 (top) and F2 (bottom)**

Simulated and observed soil water content values for the two fields are shown in Figure 8. Dotted and solid lines represent the observed and simulated values, respectively. Results show that the simulation was in good agreement with the general trend of the observed data. The simulated soil water content ( $\theta$ ) values fitted well with observed soil water content ( $\theta$ ) values. As described, the

presence and absence of tile drainage were considered in the simulation process. Soil moisture content fluctuates during the cropping season. There was an increase to complete saturation after every irrigation event, followed by a gradual decrease in soil moisture content during the following few days. Fluctuations were minimal in deep depths, and simulations showed no variations in water content. While near the soil surface, where water uptake by roots and evapotranspiration occurred, noticeable soil moisture content variations occurred.

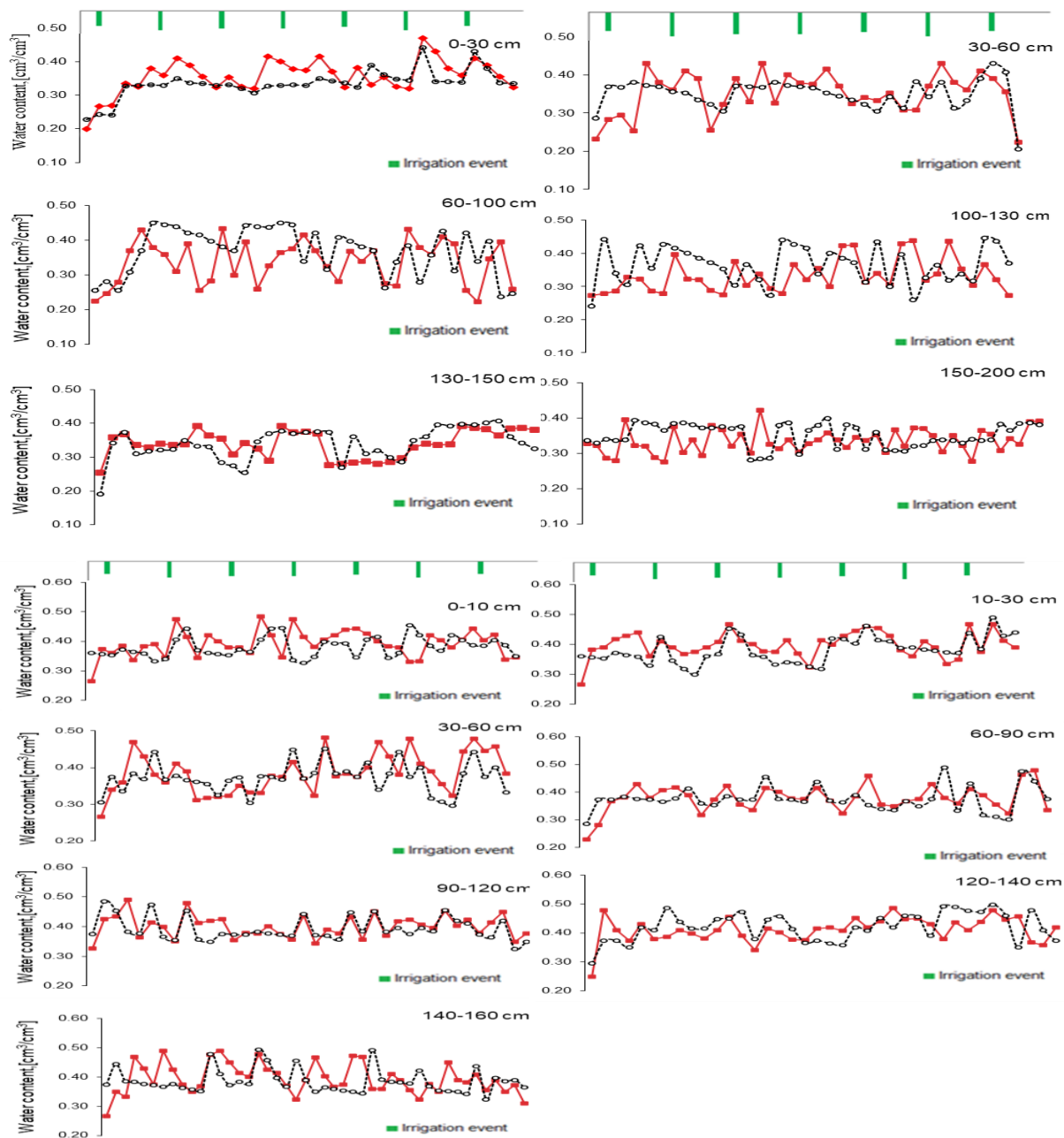


**Figure 8. Observed (dotted line) and simulated (solid line) soil water contents during the cropping season in F1 (top) and F2 (bottom)**

A simulation scenario was considered to simulate the effect of water reuse in irrigation. The scenario assumed the mixing ratio between fresh and drainage water to be 1:3 instead of 1:1. This scenario was proposed since water shortage is becoming very pronounced in the Egyptian water sector. The assumption was based on water supply augmentation.

Figures 9 and 10 show the simulation distribution results of soil salinity in F1 and F2 through the cross-section used to run the model (see figure 1 (c)). The model ran for the whole cropping season. For F1, salinity levels in the upper 70 cm soil layer varied through simulations, while the variations were less evident for deeper soil layers. Soil salinity at the top layers at the beginning of the simulation period in the current situation ranged from 0.91 to 1.03 dS / m at the soil surface and 1.67 to 2.59 dS / m at 70 cm soil depth in the scenario of change in mixing ratio (Figure 9 (a)). After 20 days of simulation, salinity at the soil surface in the current situation increased from 1.06 to 2.36 dS / m and from 1.89 dS / m to 3.50 at 70 cm soil depth in the scenario of change in mixing ratio (Figure 9 (b)). At the end of the simulation period, salinity at the soil surface in the current situation increased from 0.93 to 1.28 dS / m and from 1.09 to 2.16 dS / m at 70 cm soil (Figure 9 (c)). In the middle of the modelled domain, salinity changed gradually during the season. In the current situation, it changed from 2.87, 3.4 and 2.36 dS / m, while in the scenario change in mixing ratio, it changed from 5.19, 4.31 and 2.16 dS / m at the beginning of the simulation (Figure 9 (a)), 20 days of simulation (Figure 9 (b)) and at the end of the simulation period (Figure 9 (c)), respectively. Soil salinity levels changed in deep soil layers. In the current situation, salinity varied from 2.37, 2.97 and 1.28 dS / m and in the scenario, the change in mixing ratio was 2.38, 3.45 and 2.16 dS / m at the beginning of the simulation (Figure 9 (a)), 20 days of simulation (Figure 9 (b)) and at the end of the simulation period (Figure 9 (c)), respectively.

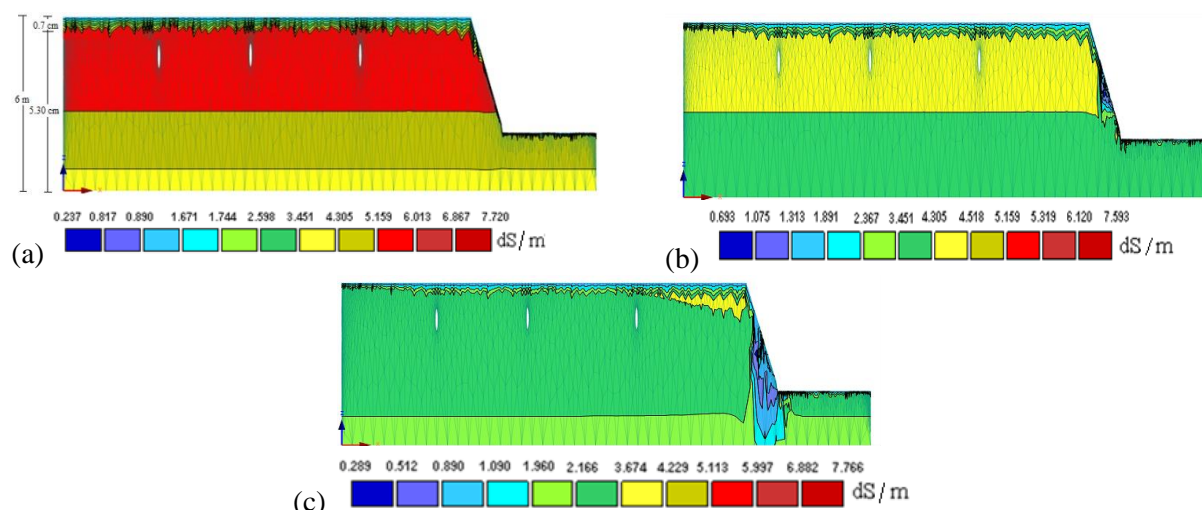


**Figure 9. Simulated distributions of the electrical conductivity of the soil solution salinity (a) at the beginning of the simulation, (b) 20 days of simulation, (c) end of simulation period in field F1 (mixing ratio of fresh to drainage water is 1:3)**

For field F2, variations were minor in the whole domain (Figure 10). Soil salinity at the top layers was the same during the simulation period, ranging between 3.25 and 4.30 dS / m at 70 cm soil depths at the beginning of the simulation (Figure 10 (a)), 20 days of simulation (Figure 10 (b)) and at the end of the simulation period (Figure 10 (c)), respectively. While in the root zone and the top 250 cm soil depths, salinity levels were high during the simulation period, with 6.50 dS / m.

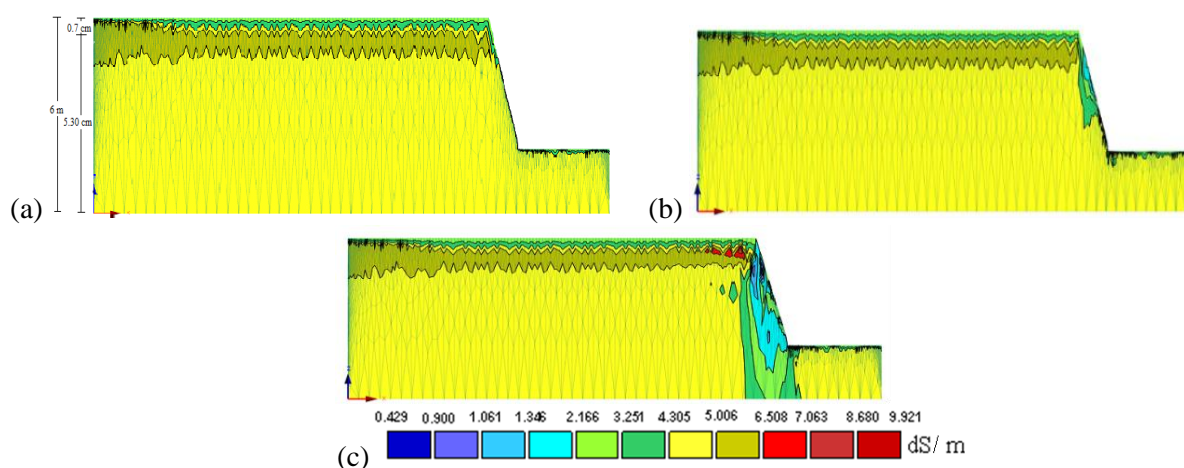


**Figure 10. Simulated distributions of the electrical conductivity of the soil solution salinity (a) at the beginning, (b) 20 days of simulation, (c) end of simulation period in field F2 (mixing ratio of fresh to drainage water is 1:3)**

For the deeper soil depths, minimal variations in salinity levels were observed with 5 dS / m, except for the parts close to the water canal. Direct use of drainage water of electrical conductivity 3 dS / m is also a common practice of some farmers in Egypt to plant several crops, e.g. wheat. Pilot studies carried out in two Governorates in Egypt showed that by applying appropriate management practices, drainage water with electrical conductivity of 2 to 2.5 dS / m could be safely used for irrigation without long-term hazardous consequences to crops or soils (FAO-48). Irrigation inevitably leads to a percolation process towards the shallow subsurface aquifer. Hence, a rise in the groundwater table causes upward vertical flows of water and salts that clog agricultural soils and produce excessive salinization, further accentuating evaporation processes. After a few years of exploitation, the degradation of soils is undoubtedly linked to this transfer of salts between groundwater and the soil (Gning et al., 2021).

## CONCLUSIONS

The presence and absence of tile drainage were considered in the simulation process. Observed and simulated data revealed that salinity increased in the root zone during the crop season under irrigation with mixed water from the irrigation canal and the surface drain. Soil moisture content fluctuated throughout the cropping season, with an increase to complete saturation after every irrigation event, followed by a gradual decrease in soil moisture content during the following days. Fluctuations were minimal in large depths, and simulations did not show variations in soil water content. While near the soil surface, where water uptake by roots and evapotranspiration occurred, noticeable soil moisture content variations occurred.

Simulation results showed that HYDRUS 2D could simulate the soil moisture contents and solute transport of both fields in this study. The model was reasonably calibrated, and subsequently, management scenarios corresponding to the deficit and over-irrigation regimes could be performed utilizing the parameterized model.

Results of the soil salinity distribution during cropping season in both fields showed that soil salinity was higher in F2 than in F1. Change in soil salinity was more pronounced in the upper soil layers, while the change in soil salinity in the more significant depths was minimal in both fields. Tile drains have helped reduce salts' effect in the root zone. This was found from the salinity values in field

F1, where tile drains were installed. These findings and the fact that Egypt is categorized as a water-stressed country make water reuse compulsory.

The study shows that water reuse can be practised despite the negative impacts on the surrounding environment, e.g. soil and groundwater, if mitigation actions accompany proper management practices to alleviate and minimize the negative impacts.

Improved sustainable and integrated land and water management strategies could be used as practical mitigation measures to safeguard the water system from future changes in the area. There is a need to emphasize the importance of leaching management. Cultivation of rice, despite high water consumption, leads to a significant reduction in soil salinization resulting from irrigation. The transfer of water and solutes in the subsurface of the delta follows charging-discharging and dilution-concentration cycles controlled by the global water balance. One of the more interesting options is to reuse drained saline water to irrigate salt-tolerant plants. Moreover, reduce the cropping intensity, e.g., cultivate crops of high market value and eliminate those of lower market value to reduce salt accumulation and save water. It is recommended to (i) carry out long-term simulations (accompanied by field experiments) and (ii) upscale plot level measurements and estimates to landscape scale.

## REFERENCES

Abrol, I.P., Yadav, J.S.P., and Massoud, F.I. (1988). Salt-Affected Soils and their Management. Food and Agriculture Organization of United Nations, Rome, Italy, Pages: 131.

Abdel-Maksoud, B. M. (2018). Estimation of air temperature and rainfall trends in Egypt. Asian Journal of Advanced Research and Reports, 1-22.

Allen, R. G., Pereira, L. C., Raes, D., and Smith, M. (1998). Crop evapotranspiration. Guidelines for computing crop water requirements, pp. 1-300, FAO Irrigation and Drainage paper 56, FAO, Rome.

Attwa, M., Gemail, K. S. and Eleraki, M. (2016). Use of salinity and resistivity measurements to study the coastal aquifer salinization in a semi-arid region: a case study in northeast Nile Delta, Egypt. Environmental Earth Sciences, 75(9), 784.

Awadallah, A. G., Magdy, M., Helmy, E. and Rashed, E. (2017). Assessment of rainfall intensity equations enlisted in the Egyptian code for designing potable water and sewage networks. Advances in Meteorology, 2017.

Christen, E. W., and Ayars, J. E. (2001). Subsurface drainage system design and management in irrigated agriculture: Best management practices for reducing drainage volume and salt load. Technical Report 38-01, CSIRO Land and Water, Griffith, NSW, Australia, 129 pp.

EGSA, Egyptian General Survey and Mining, (1997). Topographical Map cover Nile Delta, Scale 1: 2 000 000.

FAO (1998). Rome Declaration on World Food Security and World Food Summit Plan of Action (available at [www.fao.org/docrep/003/w3613e/w3613e00.htm](http://www.fao.org/docrep/003/w3613e/w3613e00.htm)).

Farid, M. S. (1980). Nile Delta groundwater study. M. Sc. thesis, Cairo University, Egypt.

Farid, M. S. (1985). Management of Groundwater System in the Nile Delta. Ph. D. thesis, Faculty of Engineering, Cairo University, Egypt.

Feddes, R. A., Kowalik, P. J., and Zaradny, H. (1978). Simulation of field water use and crop yield. pp. 1-189, Simulation Monographs, Pudoc, Wageningen.

Gning, A. A., Orban, P., Malou, R., Wellens, J., Derouane, J., Gueye, M. and Brouyere, S. (2021). Impacts of Irrigation Water on the Hydrodynamics and Saline Behavior of the Shallow Alluvial Aquifer in the Senegal River Delta. *Water*, 13(3), 311.

Hoffman, G. J., Rhaodes, J. D., Letey, J., and Fang Sheng (1990). Salinity management. Chapter 18 of Management of Farm Irrigation Systems published by ASAE.

Kotb, T. H. S., Watanaba, T., Ogino, Y., and Nakagiri, T. (2000). Soil salinization in the Nile Delta and related policy issues in Egypt, *Agr. Water Manage.*, 43, 239–261.

MALR. (2012a). Bulletin of Agricultural Statistics, Part 1 Winter crops, 2011/2010. Cairo: Ministry of Agriculture and Land Reclamation, Economic Affairs Sector

MWRI. (2014). "Water Scarcity in Egypt". Ministry of Water Resources and Irrigation in Egypt (MWRI).

MWRI. (2016). Ministry of Water Resources and Irrigation Procedures for Rainwater Management.

Negm, A. M., Abd-Elaty, I. and Abd-Elhamid, H. F. (2018). Groundwater in the Nile Delta, © Springer International Publishing AG 2018(Hdb Env Chem, DOI 10.1007/698\_2017\_193).

Page, A. L., Miller, R. H., and Keeney, D. R. (1982). Methods of Soil Analysis. Part 2. Chemical and Microbiological Properties. American Society of Agronomy. In Soil Science Society of America, Vol. 1159.

Rembold, F., Carnicelli, S., Nori, M., and Ferrari, A. (2000). Use of aerial photographs, Landsat TM imagery and multidisciplinary field survey for land cover change analysis in the lakes region (Ethiopia). *Int. Appl. Earth Observation and Geoinformation*, 2(3-4), 181- 189.

Richards, A. F. (1931). Capillary conduction of liquids through porous media. pp. 318-333 *Physics 1*.

Richards, L. A. (1954). Diagnosis and improvement of saline and alkali soils. pp. 1-160 *Agriculture Handbook*. United States Department of Agriculture.

Richards, L. A., Gardner, W. R., and Ogata, G. (1956). Physical processes determining water loss from soil. *Soil Sci. Soc. Am. Proc.* 20:310-314.

RIGW (1992). Research Institute for Groundwater, Hydrogeological Map of Nile Delta, Scale 1: 500,000, 1st Edn., Nile Delta.

RIGW (2003). Monitoring of groundwater microbiological activities in the Nile Delta aquifer. A study completed for the National Water Quality and Availability Management project (NAWQAM), Kanater El-Khairia, Egypt.

RIGW (2010). The Annual Technical report for year 2010. Research Inst. for Groundwater, Kanater El-Khairia, Egypt.

Ritzema, H. and Schultz, B. (2011). Optimizing Subsurface Drainage Practices in Irrigated Agriculture in the Semi- Arid and Arid Regions: Experiences from Egypt, India and Pakistan. *Irrigation and Drainage*, 60(3), 360-369.

Rhoades, J. D., Kandiah, A., and Mashali, A. M. (1992). The use of saline waters for crop production. FAO Irrigation and Drainage paper 48, Rome.

Stanley, D., (1996). Nile Delta: extreme case of sediment entrapment on a delta plain and consequent coastal land loss. *Marine Geology*, 189-195 pp.

Sestini, G. (1992). Implications of climatic changes for the Nile delta, *in* Jeftic, L., Millimam, J. D., and Sestini, G., eds., *Climate Change and the Mediterranean*: London, Edward Arnold, p. 535–557.

Sherif, M. M., and Singh, V. P. (1997). *Groundwater Development and Sustainability in the Nile Delta Aquifer*. Final report submitted to Binational Fulbright Commission, Egypt.

Šimůnek, J., Sejna, M., and van Genuchten, M. T. (1998). The HYDRUS-1D software package for simulating the one-dimensional movement of water, heat and multiple solutes in variably saturated media. Version 2.0, pp. 1-177. US Salinity Laboratory, Agricultural research service, US department of agriculture, Riverside, California.

Šimůnek, J., Jacques, D., Hopmans, J. W., Inoue, M., Flury, M., and van Genuchten, M.Th. (2002). Solute transport during variably saturated flow inverse methods. p. 1435–1449. J.H. Dane and G.C. Topp (ed.) *Methods of soil analysis*. Part 4. Physical methods. SSSA Book Ser. 5. SSSA, Madison, WI.

Šimůnek, J., Sejna, M., Van Genuchten, M.T. 2006. *The HYDRUS Software Package for Simulating Two- and Three-Dimensional Movement of Water, Heat, and Multiple Solutes in Variably-Saturated Media, User Manual, Version 1.0*. University of California-Riverside Research Reports. 161 pp.

Warner, J. W., Gates, T. G., Attia, F. A., and Mankarious, W. F., 1991. Vertical leakage in Egypt's Nile 15 Valley: Estimation and implications. *Irrig. J.: Drain Eng.-ASCE*, 117, 515–533.

Wolf, P. (1987). The problem of drainage and its solution in the Nile Valley and Nile Delta. *Natural Res. Develop.*, 25, 62–73.